Physics AUC, vol. 22, 50-62 (2012)

Analysis of Zirconia Thin Films Grown by Pulsed Laser Deposition

V. N. Cancea[1], R. Birjega[2], V. Ion[2], M. Filipescu[2], M. Dinescu[2]

[1]Department of Physics, University of Craiova 200585, Romania

[2]Department of Lasers, National Institute for Laser, Plasma and Radiation Physics, 077125 Magurele, Romania

Abstract

Zirconia thin films have been grown on silicon (100) substrates masked or not with photoresist by pulsed laser deposition (argon fluorine, wavelength 193 nm, repetition rate 40 Hz) of a ceramic ZrO_2 target under various treatments, like substrate temperature, presence or not of background gas, number of applied laser pulses during ablation, value of the laser fluence, laser energy per pulse, and RF-plasma assistance. The structure of the emerging thin films has been characterized by X-ray diffraction done with a PANalytical's X'Pert PRO MRD system and the optical properties have been performed by spectro-ellipsometry with a Woollam V-VASE device.

PACS: 81.05.-t, 81.15.Fg, 61.05.-a, 61.05.cp, 68.35.Ct, 78.66.-w

Keywords: zirconia thin films, pulsed laser deposition, X-ray diffraction, spectro-ellipsometry.

1 Introduction

Metal oxides are interesting materials which exhibit an extremely wide range of physical and chemical properties. They are used in a variety of technical applications that includes uses in catalysis, photocatalysis, solar panels, gas sensors, as protective or optical coatings, in biocompatible materials, in Li-based batteries, electrochromic devices, and as potential gate insulators for the new generation of MOSFETS. The surface and interface properties of metal oxides play a role in all these applications, and sometimes even dominate device performance. Among them, zirconia (zirconium dioxide) plays an important role due its high melting point, high corrosion resistance, elevated hardness, and, most important and of raised interest lately, due to its biocompatibility. Zirconia is also a good candidate for replacing SiO_2 as gate dielectric because of its dielectric constant of about 20, good thermodynamic stability with the Si wafer, low-leakage-current level, high thermal stability [1, 2, 3]. Pure ZrO_2 is known to exist as three polymorphs at different temperatures: monoclinic, tetragonal, and cubic [4].

One of the convenient ways to analyze physical and chemical properties of zirconia is to initially grow such material on thin films by various, laser or non-laser methods, made under precise and repeatable conditions. Laser ablation or Pulsed Laser Deposition (PLD) was proved to be a laser based method to grow thin films, presenting many advantages (clean method, allows deposition of compounds with complex stoichiometry,

high deposition rates). The PLD technique involves the interaction of a laser beam with a target material (solid or liquid) producing a plume which transports the particles onto a substrate, where a thin film is formed [5]. The main advantage of the PLD deposition technique consists in its quasi-universal potential in the sense that it is in principle applicable for obtaining materials of practically any type, meanwhile ensuring the precise control of the thin film thickness and an improved adherence of the synthesized material to the substrate [6, 7].

In this paper we investigate zirconia thin films that have been grown on silicon (100) or silicon masked with photoresist substrates by pulsed laser deposition (argon fluorine, λ=193 nm, ν=40 Hz) of a ceramic ZrO_2 target treated with Hafnium 2.5% under various conditions and treatments, like substrate temperature, presence or not of background gas, number of applied laser pulses during ablation, value of the laser fluence (energy density), laser energy per pulse, and RF-plasma assistance. The structural characterization of the resulting zirconia thin films has been done by X-ray diffraction (PANalytical's X'Pert PRO MRD system) and the optical characteristics have been carried out by spectro-ellipsometry (Woollam V-VASE device). XRD investigations [8] emphasized the specific conditions and treatments that favor the formation of more thermodynamically stable crystallization phases. Spectro-ellipsometry analyses [9, 10] made possible the identification of the factors that enable desired features of zirconia thin films, such as increased values of the refractive index, lower values of the extinction coefficient, and improved domain of film thickness.

2 Experimental setup

Zirconia thin films have been grown from a ceramic target of ZrO_2 treated with Hafnium 2.5%. The argon-fluoride laser beam (λ=193 nm, ν=40 Hz) has been focused on the target via a spherical lens under an angle of 45° [11, 12, 13, 14]. The laser fluence has been established in the range of 2.0 to 3.4 J·cm^{-2}. In order to render a uniform ablation the target has been simultaneously translated and rotated [15]. Two different substrates have been employed: pure Si(100) and respectively Si(100) masked with photoresist. These substrates have been placed at a distance of 4 cm from the target, parallel to the target. The substrates have been heated up to a temperature within 300° – 600° C. The pulsed laser depositions (PLDs) have been done in vacuum and respectively in presence of oxygen background at 0.01 mbar. Some films have been grown by radio-frequency PLD, in which case the power of the RF beam has been maintained at 100 W [16].

A major problem encountered in the growth of complex oxides is the appearance of oxygen vacancies both inside the layer and at the layerâ€"substrate (bottom electrode) interface. To avoid this problem, a complex RF-PLD system was used, which combines the advantages of conventional PLD (on step process synthesis and deposition, spatial control of the deposited laser energy, use of simple and non-hazardous chemical compounds, low-temperature and high-efficiency process) with *in situ* enhancement of the reactivity on the substrate due to the presence of an reactive beam of oxygen species. In this way, during the growth process both the species originated from laser plasma plume (Zr oxides, ions, etc.) and oxygen species generated by the RF discharge contribute to form the zirconium oxide molecules. The plasma beam source consists in a double-chamber discharge system supplied by a RF (13.56 MHz, CESAR 1310, RF maximum power 1000 W) power supply. The discharge is generated in the active chamber in flowing oxygen between two parallel electrodes: it expands into the ablation chamber as a plasma beam through an aperture performed in the bottom electrode, which acts as a nozzle. The experimental setup is

summarized in Table 1.

Sample	Target	Substrate	P (mbar) during deposition	d_{t-s} (cm)	$T_{substrate}$ (°C)	E_{laser} (mJ)	N_{pulses}	Spot area (mm^2)	Φ_{laser} (Jcm^{-2})	P_{RF} (W)	λ (nm)
1157	ZrO_2	Si + Si photore-sist	vacuum	4	room	17	40,000	0.5	3.4	0	193
1158	ZrO_2	Si	vacuum	4	300	17	80,000	0.5	3.4	0	193
1159	ZrO_2	Si	vacuum	4	600	17	80,000	0.5	3.4	0	193
1160	ZrO_2	Si	0.01 O_2	4	room	17	80,000	0.5	3.4	0	193
1161	ZrO_2	Si	0.01 O_2	4	300	17	80,000	0.5	3.4	0	193
1162	ZrO_2	Si	0.01 O_2	4	600	17	80,000	0.5	3.4	0	193
1163	ZrO_2	Si	0.01 O_2	4	room	17	80,000	0.5	3.4	100	193
1164	ZrO_2	Si	0.01 O_2	4	300	10	80,000	0.5	2.0	100	193
1165	ZrO_2	Si	0.01 O_2	4	300	17	80,000	0.5	3.4	100	193
1166	ZrO_2	Si	0.01 O_2	4	600	17	80,000	0.5	3.4	100	193

Table 1: Experimental setup for growing ZrO_2 thin films.

Next, the emerging thin films have been characterized via two main techniques, namely X-ray diffraction and spectro-ellipsometry.

3 Results and discussions

3.1 X-ray diffraction

X-ray diffraction (XRD) represents a non-destructive method that provides information on the crystalline structure, chemical composition, and various physical properties of both materials and thin films. This scattering of an X-ray beam that hits a sample technique is based on observing the scattered intensity as a function of three parameters, namely incident and scattered angle, polarization, and wavelength or energy.

X-rays is a form of electromagnetic radiation with the photon wavelengths in the range of 0.01 to 10 nm and energies in the range of 100 eV to 100 keV. For diffraction purpose there are used only short wavelengths X-rays in the range of a few ångströms up to a tenth of an ångström or, equivalently with the energy between 1 keV and 120 keV. Since the wavelengths of X-rays are similar to the size of atoms they are also useful for determining the crystalline structures of atoms and molecules in a wide variety of materials. The main X-ray source is an X-ray tube, a vacuum tube that uses a high voltage to accelerate the electrons released by a hot cathode to a high velocity. The resulting focused beam of accelerated electrons hits a solid target and thus generates X-rays. When the electrons hit the target, X-rays are created by two different atomic processes: X-ray fluorescence (this process produces an emission spectrum of X-rays at a few discrete frequencies, known as spectral lines) and Bremsstrahlung (the radiation given off by the electrons as they are scattered by the strong electric field near the high-Z nuclei). In the case of Bremsstrahlung the electrons decelerate as a consequence of their deflection by the atoms from the target and these X-rays have a continuous spectrum.

An X-ray diffractometer is equipped with an *in situ* temperature chamber for the investigation of temperature dependent phase transition of the sample and an ultrafast detector for real-time acquisition of structural data and within the simulation conditions applied during the growth or post-synthesis treatments of thin films.

There are many physical parameters, such as the substrate temperature, the heating or cooling rate, the gas pressure or the gas composition — during the growth and/or post-deposition treatments — that may become leading monitoring parameters in respect with thin film composition, quality, and reproducibility (the act of repeating a particular thin film deposition). These monitoring parameters allow the investigation of the evolution of various crystallographic or polymorphic phases, phase transitions, internal and residual stresses induced by thermal treatment, evolution of thin film â€“ substrate interface, and texture of the deposited thin films. (By thin film texture it is understood the distribution of crystallographic orientations of a poly-crystalline sample. A sample in which these orientations are fully random is said to have no texture. If the crystallographic orientations are not random, but have some preferred orientation, then the sample has a weak, moderate, or strong texture. The degree is dependent on the percentage of crystals having the preferred orientation.) In the meantime the acquisition of structural data, such as dilatation or contraction or internal stress of crystal lattices — related to the substrate behavior under some temperature and pressure conditions similar to those existing during the deposition process, improve the understanding of thin film growing mechanism on various substrates.

The structural XRD analysis of all thin film structures presented in this paper has been performed with a PANalytical's X'Pert PRO MRD (Materials Research Diffractometer) system with standard $\theta - 2\theta$ Bragg-Brentano diffraction geometry. X-ray Diffraction on ZrO_2 thin films shows at what extent the deposition conditions influence on the crystal structure of deposited thin films.

From Fig. 1 it is clear the dependence of thin film cristallinity on the substrate temperature, in the sense that the higher the temperature the more accurate the crystal phase. While for films deposited at room temperature only an amorphous peak around $2\theta = 30°$ is observed, for films grown at 300° C there appear broad diffraction maxima, not so clearly defined, accredited to the tetragonal crystal phase of ZrO_2 and respectively to the (-111) reflection of monoclinic ZrO_2 phase. On the contrary, for films grown at 600° C the two crystal phases [tetragonal and respectively (-111) reflection of monoclinic ZrO_2] exhibit a long-range crystal organization. It can be concluded that the tetragonal phase is dominant for the films deposited at 600° C, while for those deposited at 300° C the fraction of monoclinic phase is prevailing.

For the samples prepared under radio-frequency (RF) sputtering at a temperature of 600° C it is observed the formation of the same two ZrO_2 crystal phases as before — tetragonal and monoclinic (see Fig. 2) — but with an obvious increase in the proportion of monoclinic phase, which is thermodynamically more stable. More maxima pertaining to the monoclinic phase have been recorded within the diffraction spectrum of thin films deposited in the presence of RF, suggesting the formation of a polycrystalline monoclinic phase.

Figure 3 displays the comparative analysis of X-Ray spectra for ZrO_2 samples deposited at the same substrate temperature of 600° C in presence of oxygen background at 0.01 mbar and respectively in vacuum. In the case of vacuum conditions one observes the formation in a leading proportion of a tetragonal phase in which the (002) reflection is also visible. The monoclinic maximum (-111) is less intense, so one can conclude that vacuum conditions are best for obtaining the largest fraction of tetragonal phase.

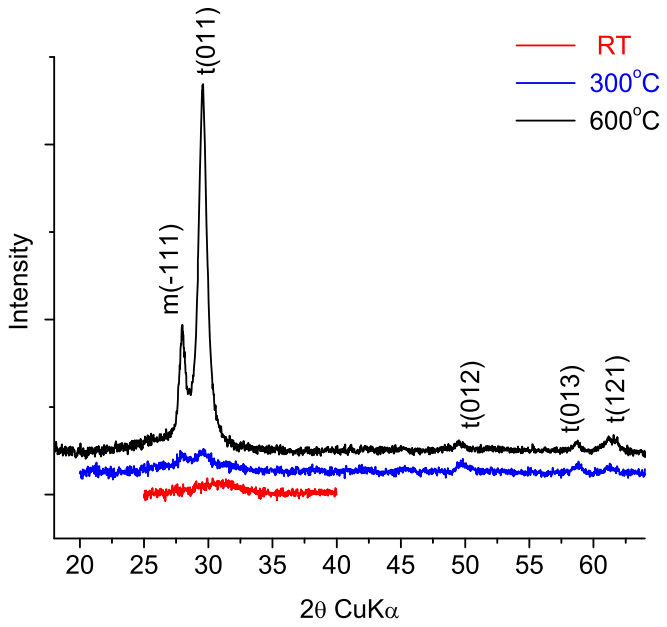

Figure 1: X-ray diffractograms of ZrO_2/Si(100) thin films deposited at various substrate temperatures.

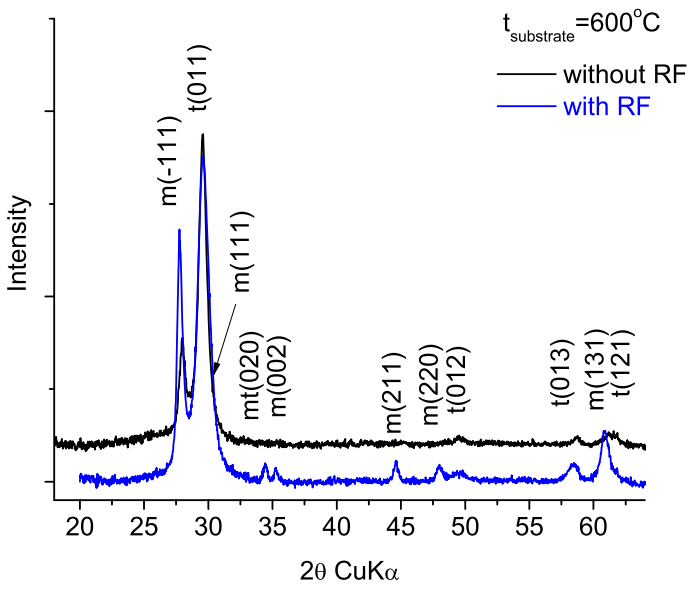

Figure 2: X-ray diffractograms of ZrO_2/Si(100) thin films deposited at 600°C with and without RF.

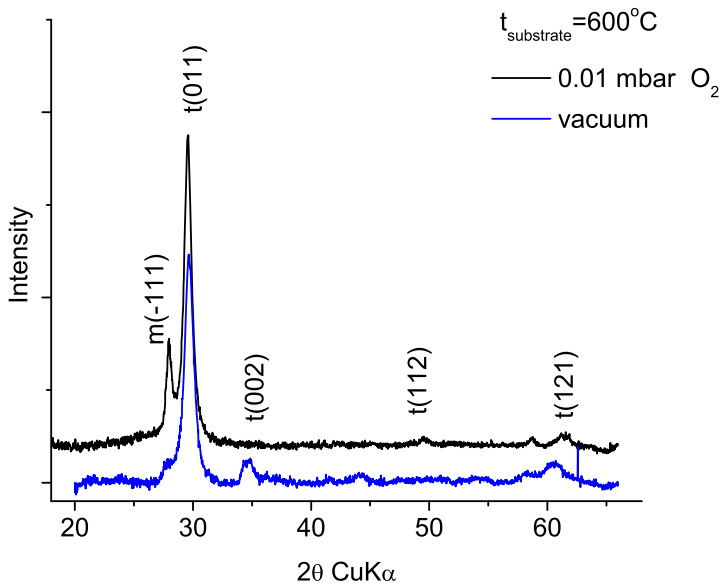

Figure 3: X-ray diffractograms of ZrO_2/Si(100) samples deposited at 600°C in vacuum and respectively in presence of O_2 background at 0.01 mbar.

3.2 Spectro-ellipsometry

Spectro-ellipsometry is an experimental technique used to detect the change in the polarization ρ of a light beam reflected or transmitted from a surface sample. The polarization change is represented as the change in amplitude ratio Ψ and change in phase shift Δ, respectively between the p- and s- components of the light beam's electric field. These two parameters are defined via the ratio between the Fresnel reflection coefficients R_{p} and R_{s} respectively corresponding to the polarizations p and s of the electric fields parallel and respectively orthogonal to the incidence plane:

$$\rho = \frac{R_{\mathrm{p}}}{R_{\mathrm{s}}} = (\tan \Psi) \exp (i\Delta). \tag{1}$$

The measured response in ellipsometry depends on the optical properties and thickness of individual materials [9, 10].

Data analysis proceeds as follows: After a sample is measured, an optical model is constructed to describe the sample. The model is used to calculate the predicted response from Fresnel's equations (theoretical curves for the parameters Psi Ψ and Delta Δ), which describe each material with thickness and optical constants. The calculated values are then compared to the experimental data. Finding the best match between the model and the experiment is typically achieved through regression. An estimator, like the Mean Squared Error (MSE), is used to quantify the difference between curves. The unknown parameters are allowed to vary until the minimum MSE is reached. The best answer corresponds to the lowest MSE. In the case of thin films deposited by various techniques on a collecting material the optical model is usually composed of a chosen number of layers of material [9, 10].

The experimental data of Psi and Delta have been measured with a Woollam V-VASE spectroellipsometer equipped with a HS-190 monochromator in the spectral range of 250

to 1700 nm, in steps of 2 nm, and at incident angles of the light beam of 60°, 65°, and 70°.

For zirconia thin films prepared by RF-plasma-assisted PLD on Si(100) substrates the theoretical optical model comprises: the silicon substrate, a layer of native oxide of silicon of approximately 3 nm in thickness, the ZrO_2 thin film, and a roughness layer. The composition of the rough layer was approximated to 50% zirconia and 50% air, for ease of calculation.

The calculation of the refractive index (n), extinction coefficient (k), thickness, and roughness of the investigated zirconia thin films from the recorded experimental data required a two-step fitting procedure. In the first step there were identified the film thickness and the intermediate values of n for a specific spectral range of 500 to 1700 nm, within which zirconia is practically transparent [17] (does not absorb photon radiation at this values of the wavelength, so the extinction coefficient can be taken to vanish, $k = 0$). The refractive index n of the ZrO_2 films was modeled using a Cauchy-type dispersion relationship (Cauchy fitting) [9, 10]

$$n(\lambda) = A_n + \frac{B_n}{\lambda^2} \qquad (k = 0). \tag{2}$$

Finally, the MSE between the experimental and fitted data was calculated for all the six investigated samples. The resulting values of the Cauchy parameters A_n and B_n together with thickness and roughness values for all the investigated zirconia samples, and also the MSE results, are given in Table 2.

It can be observed that the MSE values are sufficiently low for most of the investigated samples (five out of the six investigated), so the used Cauchy fitting is acceptable. Nevertheless, for the sample 1159 (vacuum-deposited zirconia) the MSE value is high and accordingly the roughness displays bad values.

Sample	Thickness (nm)	Roughness (nm)	A_n	B_n	MSE
1159	132.954 ± 0.355	0.000 ± 0.702	2.0641 ± 0.00401	0.050961 ± 0.00338	50.05
1162	59.009 ± 0.0439	2.458 ± 0.0736	2.1821 ± 0.000991	0.014426 ± 0.000251	2.176
1163	64.177 ± 0.0391	0.904 ± 0.06	1.9882 ± 0.000591	0.014203 ± 0.000156	1.908
1164	55.309 ± 0.0512	3.324 ± 0.0809	2.1574 ± 0.00111	0.01744 ± 0.000243	1.784
1165	190.812 ± 0.0537	1.403 ± 0.0481	2.1417 ± 0.000256	0.018515 ± 0.000153	5.944
1166	154.380 ± 0.0384	2.047 ± 0.0429	2.1535 ± 0.000211	0.01856 ± 0.000192	4.815

Table 2: Cauchy parameters for ZrO_2/Si(100).

The second step is more difficult and assumed data fitting on the entire spectral domain of 250–1700 nm. Due to the Cauchy model limitations (valid only within the transparency range), we adopted a new model — based on a Gauss oscillator — in the framework of which the correct values of the refraction and extinction coefficients on the overall interval can be determined. The Gaussian oscillator fitting method relates to the description of optical properties in terms of dielectric functions [9, 10]

$$\varepsilon_2(E) = A\left\{\exp\left[-\left((E - E_n)/\sigma\right)^2\right] - \exp\left[-\left((E + E_n)/\sigma\right)^2\right]\right\}, \tag{3}$$

where A is the amplitude of the curve's peak, E_n refers to the centering energy or energy at the curve's peak, and σ is the standard deviation of the curve. The complex dielectric

description is then related to the description in terms of the complex refraction index via the standard square-type relationship [9, 10]. The values for thickness and roughness for each sample were taken from the first step and kept fixed over the entire spectral domain.

In Figs. 4 and 5 are given the experimental curves and those obtained by Gauss-oscillator fitting method for the parameters Delta Δ and Psi Ψ for the sample 1166 prepared by RF-plasma-assisted PLD on a silicon substrate at the substrate temperature of 600° C. It is clear that the two curves display the same behavior, so we can conclude from the MSE values that the Gauss oscillator fitting method was appropriate in this case.

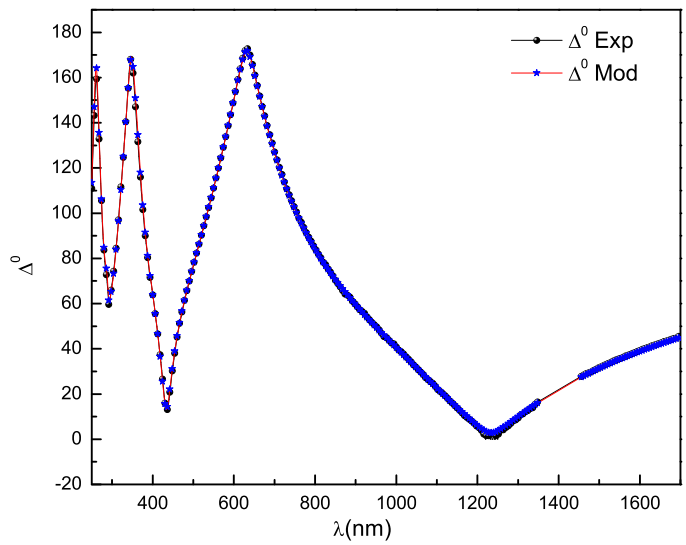

Figure 4: Experimental and Gauss-modeled curves for the parameter delta (Δ) for a ZrO_2/Si(100) thin film deposited at 600° C by RF-plasma-assisted PLD.

In Table 3 are given the values of the Gaussian parameters (Amp is the peak amplitude, En the peak energy, and Br represents the oscillator width) and again the MSE values for all the six samples investigated. They are small for all the samples excepting sample 1159. The extremely high value of MSE for this sample can be explained by presence of defects like cracks or inclusions in this zirconia thin film.

Sample	Amp	En (eV)	Br (eV)	MSE
1159	7.0779 ± 0.0894	13.966 ± 0.295	8.9853 ± 0.263	72.41
1162	13.443 ± 0.112	9.4408 ± 0.027	3.7031 ± 0.0386	5.099
1163	19.849 ± 5.15	8.9932 ± 0.137	1.9394 ± 0.525	4.533
1164	11.985 ± 0.048	9.6448 ± 0.0188	4.1471 ± 0.0225	3.786
1165	20.196 ± 1.41	8.841 ± 0.0585	2.2913 ± 0.171	9.675
1166	16.331 ± 0.338	9.1236 ± 0.0346	2.9503 ± 0.0698	9.783

Table 3: Parameters of the Gauss-oscillator fitting method for ZrO_2/Si(100).

The dependencies of the parameters n and respectively k generated by the above values

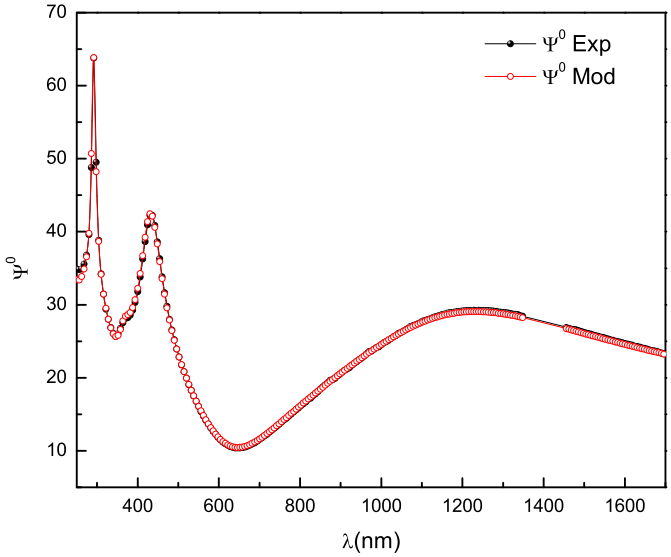

Figure 5: Experimental and Gauss-modeled curves for the parameter psi (Ψ) for a ZrO_2/Si(100) thin film deposited at 600° C by RF-plasma-assisted PLD.

of the Gauss parameters are represented in Figs. 6 and 7.

From Figs. 6 and 7 it can be concluded that higher refraction indices are obtained for zirconia thin films on silicon substrates grown at 300° C and 600° C than for those grown at room temperature. The values of the extinction coefficients are small (10^{-3}) for all samples, which show that they are practically transparent on a large spectral domain (250-1700 nm).

In the case where the PLD depositions are done at different values of the fluence, namely 2 J·cm^{-2} and respectively 3.4 J·cm^{-2}, the values of the refractive index are very close, as it can be seen from Fig. 8, although film thickness is decreasing with fluence (see Table 2). This means that the material deposition rate during the PLD process is lower at a lower value of the laser fluence.

For ZrO_2 thin films deposited on Si(100) at 600° C (see Figs. 9 and 10) there are observed lower values of the refraction index in the case of vacuum depositions compared to the depositions in oxygen backgrounds during an increase of pressure to 0.01 mbar. The values of the refractive index n are similar in the case of a simple ablation compared to RF-plasma-assisted PLD. The main difference is noticed at the level of the values of the extinction coefficient k in the sense that the RF treatment favors a less absorption of the photon beam energy.

4 Conclusions

In this paper we presented the structural and optical characterization of zirconia thin films deposited on Si(100) or silicon masked with photoresist substrates by PLD under various treatments with the help of two main analysis techniques: X-ray diffraction and spectro-ellipsometry. XRD investigations emphasized that a high temperature of the substrate during the deposition process (600° C) corroborated with a RF-plasma-assisted treatment

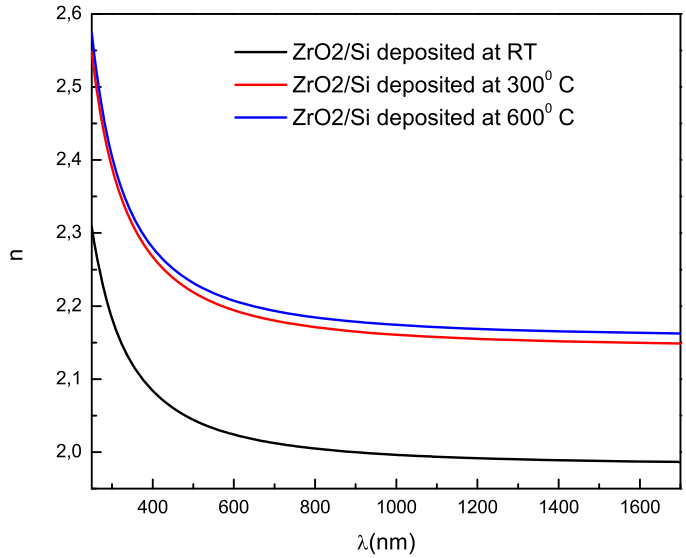

Figure 6: Dependencies of n for ZrO_2/Si(100) deposited by PLD at different temperatures.

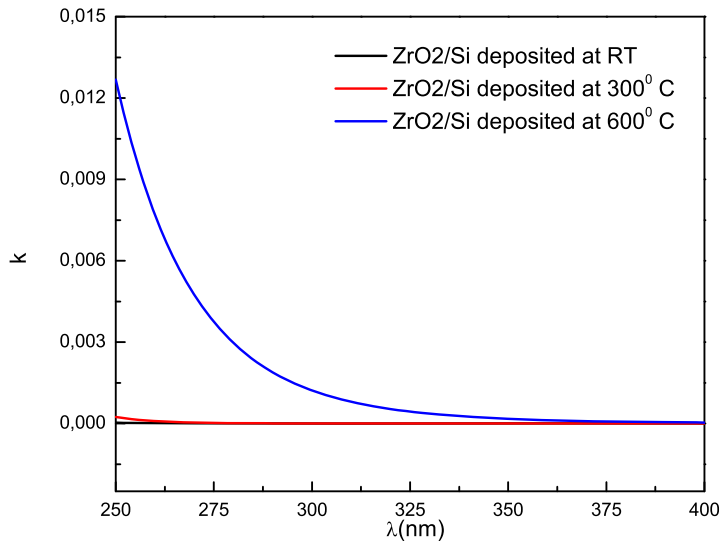

Figure 7: Dependencies of k for ZrO_2/Si(100) deposited by PLD at different temperatures.

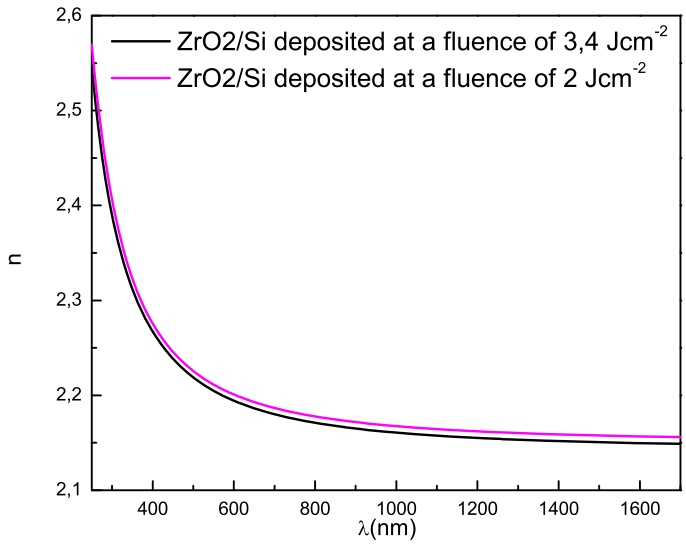

Figure 8: The dependencies of n for ZrO_2/Si(100) deposited by PLD at different fluences.

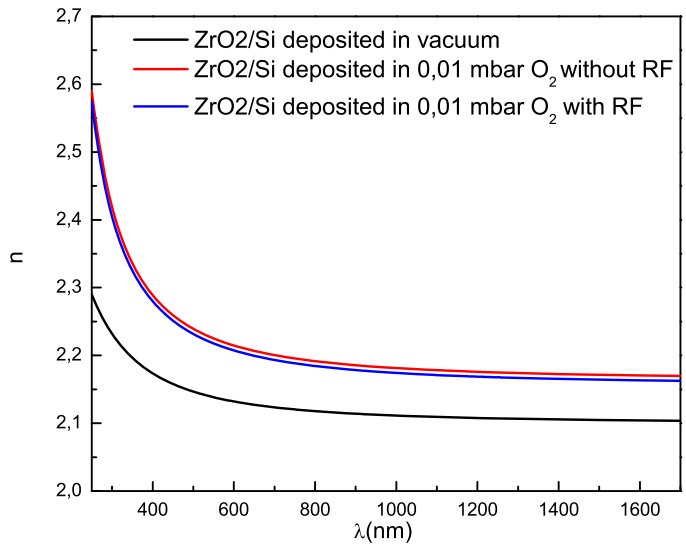

Figure 9: The dependencies of n for ZrO_2/Si(100) deposited by PLD under various conditions: in vacuum, in O_2 background, with or without RF treatment.

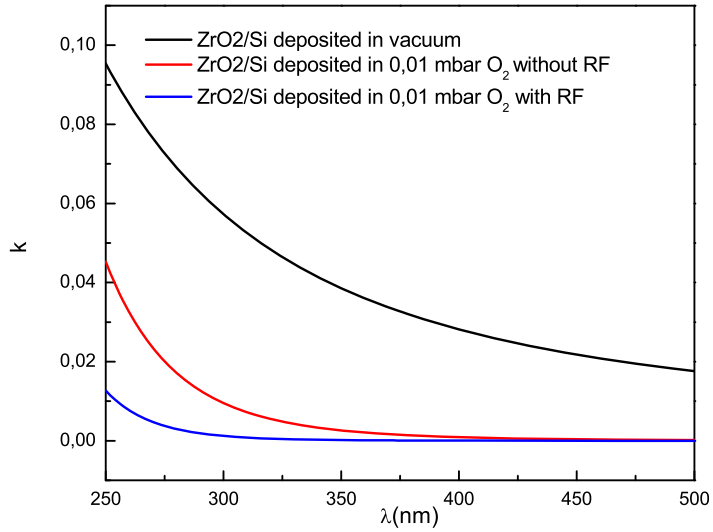

Figure 10: The dependencies of k for ZrO_2/Si(100) deposited by PLD under various conditions: in vacuum, in O_2 background, with or without RF treatment.

in a background of 0.01 mbar O_2 favors the crystallization process and leads to the formation of tetragonal and monoclinic phases, with an obvious increase in the proportion of monoclinic zirconia, which is thermodynamically more stable. In vacuum and at a substrate temperature of 600° C it is observed a clear dominance of the tetragonal phase over the monoclinic one. Regarding the spectro-ellipsometry investigation of ZrO_2/Si(100) thin film samples deposited by PLD, we showed that in the given experimental setup it is possible to build a correct optical model, based on a two-step fitting procedure that involves Cauchy and respectively Gauss-oscillator fitting methods. The main conclusions that can be drawn from the recorded experimental data are that a higher temperature of the substrate and respectively of the background gas (O_2) pressure during the deposition process favors a higher value of the refractive index, film thickness is decreasing with the fluence, so the material deposition rate during the PLD can be improved by a higher laser fluence, and finally, the supplementary treatment of ZrO_2 thin films by RF-plasma-assistance helps at obtaining lower values of the extinction coefficient, and therefore the desired feature of such materials to absorb photon beam energy as low as possible.

Acknowledgments

One of the authors (V.N.C.) acknowledges partial support from the doctoral contract 336/9/B/30.09.2011 with the University of Craiova.

References

[1] G. D. Wilk, R. M. Wallance, J. M. Anthony, J. Appl. Phys. **89** (2001) 5243–5275

[2] K. Sasaki, J. Maier, Sol. St. Ionics **134** (2000) 303–321

[3] W. J. Qi, R. Nieh, B. H. Lee, L. Kang, Y. Jeon, J. C. Lee, Appl. Phys. Lett. **77** (2000) 3269–3271

[4] X. Zhao, D. Vanderbilt, Phys. Rev. B **65** (2002) 075105 (10 pages)

[5] D. Brodoceanu, N. D. Scarisoreanu, M. Filipescu, G. N. Epurescu, D. G. Matei, P. Verardi, F. Craciun, M. Dinescu, *Pulsed laser deposition of oxide thin films*, in Plasma Production by Laser Ablation, PPLA 2003, World Scientific (2004) 41–46

[6] H. Sankur, J. G. Nelson, A. T. Pritt Jr., W. J. Gunning, J. Vac. Sci. Technol. A **5** (1987) 15–21

[7] E. W. Kreutz, J. Gottmann, phys. status solidi (a) **166** (1998) 569–580

[8] A. Guinier, X-Ray Diffraction: In Crystals, Imperfect Crystals, and Amorphous Bodies, Dover Books on Physics, 1994

[9] H. G. Tompkins, E. A. Irene (Eds.), Handbook of Ellipsometry, William Andrew, Inc., Springer Verlag, 2005

[10] H. Fujiwara, Spectroscopic ellipsometry: principles and applications, John Wiley & Sons Ltd., 2007

[11] R. Dinu, M. Dinescu, J. D. Pedarnig, R. A. Gunasekaran, D. Bäuerle, S. Bauer-Gogonea, S. Bauer, Appl. Phys. A **69** (1999) 55–61

[12] P. Verardi, M. Dinescu, F. Craciun, Appl. Surf. Sci. **154-155** (2000) 514–518

[13] F. Craciun, P. Verardi, D. Brodoceanu, M. Morar, C. Galassi, C. Grigoriu, M. Dinescu, Mater. Sci. Semicond. Proc. **5** (2002) 227–232

[14] I. Vrejoiu, D. G. Matei, M. Morar, G. Epurescu, A. Ferrari, M. Balucani, G. Lamedica, G. Dinescu, C. Grigoriu, M. Dinescu, Mater. Sci. Semicond. Proc. **5** (2002) 253–257

[15] N. Arnold, D. Bäuerle, Appl. Phys. A **68** (1999) 363–367

[16] G. Dinescu, B. Mitu, E. Aldea, M. Dinescu, Vacuum **56** (2000) 83–86

[17] W. Zhamg, J. Gan, Z. Hu, W. Yu, Q. Li, J. Sun, N. Xu, Appl. Spectrosc. **65** (2011) 522–527